catalysts

MDPI

Article

Synthesis of Tetrahydropyran from Tetrahydrofurfuryl Alcohol over Cu–Zno/Al_2O_3 under a Gaseous-Phase Condition

Fengyuan Zhang [1,2,3], Bin Zhang [4], Xincheng Wang [1,2], Long Huang [1,2,*], Dekun Ji [1,2], Songsong Du [1,3], Lei Ma [1,2] and Shijing Lin [1,2]

1 College of Chemical Engineering, Beijing Institute of Petrochemical Technology, Beijing 102617, China; zhangfengyuan@bipt.edu.cn (F.Z.); wangxc@bipt.edu.cn (X.W.); jidekun@bipt.edu.cn (D.J.); 5320150103@bipt.edu.cn (S.D.); 0020160009@bipt.edu.cn (L.M.); linshijing@bipt.edu.cn (S.L.)
2 Beijing Key Laboratory of Fuels Cleaning and Advanced Catalytic Emission Reduction Technology, Beijing 102617, China
3 Graduate School of Beijing University of Chemical Technology, Beijing 100029, China
4 Institute of Coal Chemistry, Chinese Academy of Sciences, P.O. Box 165, Taiyuan 030001, China; zhangbin2009@sxicc.ac.cn
* Correspondence: huangl@bipt.edu.cn; Tel.: +86-010-8129-2131

Received: 24 January 2018; Accepted: 7 February 2018; Published: 6 March 2018

Abstract: Tetrahydropyran (THP) represents an O-containing hetero-cyclic compound that can be used as a promising solvent or monomer for polymer synthesis. In this work, Cu–ZnO/Al_2O_3 catalysts have been prepared by a facile precipitation–extrusion method and used for the synthesis of THP through gaseous-phase hydrogenolysis of tetrahydrofurfuryl alcohol (THFA). The effect of the molar ratio of Cu/Zn/Al, reaction temperature, and hydrogen pressure was investigated. An 89.4% selectivity of THP was achieved at 270 °C and 1.0 MPa H_2. Meanwhile, the optimum molar ratio of Cu/Zn/Al was determined to be 4:1:10. The Cu–ZnO/Al_2O_3 catalyst exhibited high catalytic activity and stability for 205 h on-stream. A possible reaction mechanism involving several consecutive reactions was proposed: THFA was firstly rearranged to 2-hydroxytetrahydropyran (2-HTHP), followed by the dehydration of 2-HTHP to 3,4-2H-dihydropyran (DHP) over acid sites; finally, the DHP was hydrogenated to THP. The synergy of acid sites and metal sites of Cu–ZnO/Al_2O_3 played an important role during the production of THP.

Keywords: tetrahydropyran; tetrahydrofurfuryl alcohol; Cu–ZnO/Al_2O_3

1. Introduction

Catalytic upgrading of biomass-derived furfural or its derivatives to value-added chemicals has received great attention in recent years [1–3]. Furfural and 5-hydroxymethylfurfural (HMF), which are considered to be promising biorenewable platform chemicals, can be derived through acid-catalyzed dehydration of hemicellulose from various abundant agricultural raw materials, such as hemicellulose grain shell, hardwood lumber, corncobs, wheatbran, and other renewable biomass materials [4–7]. There were intense studies carried out on the production of high value-added chemical intermediates and end products from HMF using heterogeneous catalysts [8–11]. Tetrahyrofurfuryl alcohol (THFA) can be obtained through hydrogenation of furfural at a very high yield [12], and from which various useful chemicals, such as 1,5-pentadiol (15PDO) [13–25], 3,4-2H-dihydropyran (DHP) [26–28], and 4-penten-1-ol can be produced [29,30]. 15PDO, via a ring closure pathway, can form tetrahydropyran (THP) through the participation of strong solid acid catalysts or high-temperature water [31]. Moreover, THP can be obtained by the hydrogenation of DHP [32]. THP can be used as both a solvent and an intermediate in the synthesis of organic compounds such as glutaric acid,

heptanediamine, 1,5-dichloropentane, and pimelic acid [32,33]. However, the synthesis of THP directly from THFA using heterogeneous catalysts is rarely reported.

Recently, the catalytic conversion of furanics has been extensively studied over noble metal catalysts. However, due to the high cost and depleting resources of noble metals, it is of great importance to explore catalytic systems over non-noble metals. Among non-noble metals, copper-based catalysts were widely used in hydrogenation and hydrogenolysis reactions due to their good catalytic performance and low cost. Müller et al. [34] found that dimethyl succinate could be completely converted to THF over CuO–ZnO/Al_2O_3 at 220/Allely MPa. Guo et al. [35] also reported that a selectivity of THF as high as 94% could be obtained over Cu-B/Al_2O_3 during the hydrogenolysis of dimethylsuccinate. The selective conversion of furanic-derived compounds over Cu catalysts is particularly encouraging and needs further investigation. Soghrati et al. [36] reported that a 70% yield of THP was achieved via hydrogenolysis of THFA over Ni/HZSM-5 catalyst, encouraging us to investigate the probability of producing THP from THFA over Cu catalysts.

In this paper, we have prepared a bi-functional Cu–ZnO/Al_2O_3 catalyst by a facile precipitation extrusion method. The physic-chemical properties were characterized by XRD, BET, TEM, NH_3-TPD, and H_2-TPR analysis. The role of Cu metal sites during the direct conversion of THFA to THP over Cu–ZnO/Al_2O_3 catalysts was studied. The effect of temperature, pressure, and catalysts on THFA to THP along with side reactions was investigated. The current work was beneficial to develop the downstreams of TFHA over non-noble catalysts.

2. Results and Discussion

2.1. Catalyst Characterization

2.1.1. BET Characterization

The porosity and pore-size distribution of the calcined Cu–ZnO/Al_2O_3 extrudate catalysts were determined by N_2 adsorption–desorption. The γ-Al_2O_3 (boehmite particles behaving as a binder and supplying acid sites) exhibited a 12 nm mean diameter (Figure S1). Accordingly, the volume-size distribution of Cu–Zn particles was characterized as a bimodal distribution with a mean diameter of 2.7 nm. The other peak resulting from 8.2 nm particles was possibly derived from symbiotic fragments. Therefore, the extrudate's pore size distribution might be related with the solid composition, because the respective catalysts particle sizes differed significantly; therefore, the effect of the amount of γ-Al_2O_3 on the main peak of the size distribution was not negligible. Lamelleted mesoporous materials exhibited a typical type-III shaped isotherm, obtained by nitrogen adsorption–desorption measurements (Figure S2). The surface areas (S_{BET}) of the calcined catalysts increased monotonically from 196.4 to 261.7 $m^2 \cdot g^{-1}$ with the increase in the content of γ-Al_2O_3, though they were generally lower than that of γ-Al_2O_3 ($A_{0\text{-}0\text{-}01}$) (Table 1). This is consistent with the study by Kraushaar-Czarnetzki et al. [34].

Table 1. The physicochemical properties of the catalysts.

Catalysts	Cu/Zn/Al Molar Ratio	SBET ($m^2 \cdot g^{-1}$)	Pore Volume ($cc \cdot g^{-1}$)	Copper Crystalline Size (nm)	Average Pore Size (nm)
$A_{4\text{-}1\text{-}00}$	4:1:00	41.3	0.18	34.4	8.8
$A_{0\text{-}0\text{-}01}$	0:0:10	310.3	0.94	-	6.1
$A_{4\text{-}1\text{-}03}$	4:1:03	196.4	0.54	26.6	4.7
$A_{4\text{-}1\text{-}05}$	4:1:05	199.3	0.61	25.8	4.5
$A_{4\text{-}1\text{-}07}$	4:1:07	203.5	0.63	25.0	3.9
$A_{4\text{-}1\text{-}10}$	4:1:10	223.8	0.68	24.3	3.8
$A_{4\text{-}1\text{-}15}$	4:1:15	261.7	0.70	22.3	3.6

2.1.2. XRD Characterization

The XRD patterns of calcined catalysts are shown in Figure 1. Diffuse diffraction peaks at 2θ = 35.5°, 38.9°, and 64.2° (JCPDS 05-0661) were attributed to crystalline CuO, and the XRD patterns were associated with the copper crystalline size and the copper species [37]. The peak intensities of both CuO and ZnO were weakened with the increase in aluminum content, possibly due to the increased dispersion of Cu and Zn species after the addition of γ-Al_2O_3 (Figure 2). The copper crystallite size of all catalysts were determined to be 34.4 nm, 26.6 nm, 25.8 nm, 25.0 nm, 24.3 nm, and 22.3 nm by the Scherrer equation, based on the full width at maximum Cu diffraction of 35.5°. The peak of γ-Al_2O_3 was not observed due to the high dispersion of γ-Al_2O_3 species.

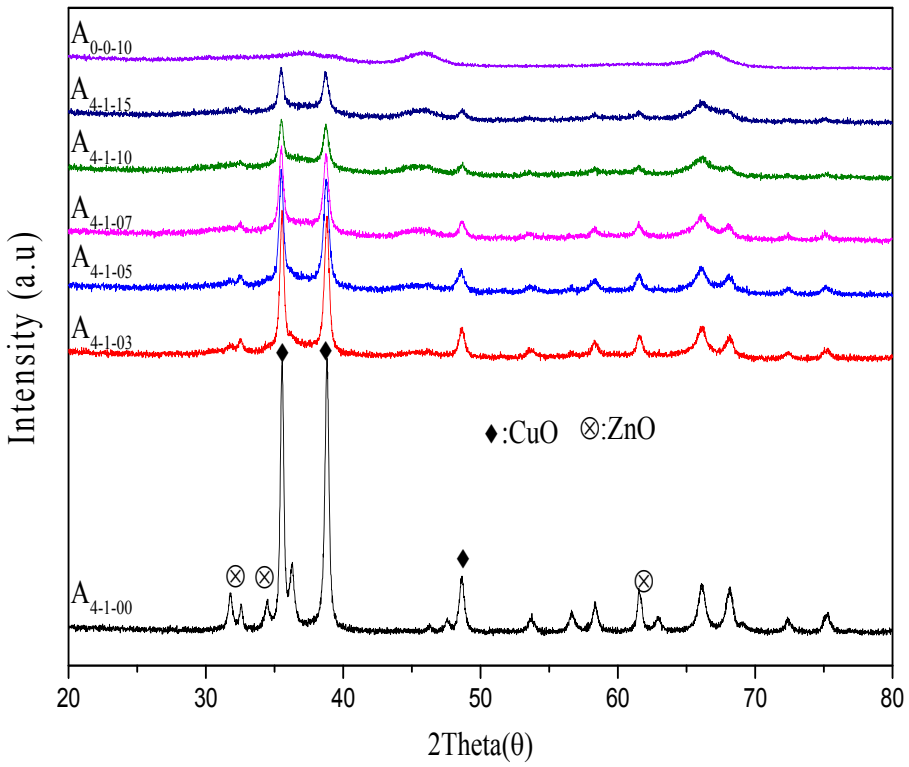

Figure 1. XRD patterns of calcined catalysts samples with different amount of γ-Al_2O_3.

2.1.3. NH_3-TPD Characterization

The acidity of samples was determined by NH_3-TPD. The acid distribution was obtained by Gaussian fitting of NH_3-TPD curves (Table 2 and Figure S3). Three peaks centered at 104 °C, 225 °C, and 335 °C were fitted for the NH_3-TPD curve, attributing to the NH_3 desorption from the weak, medium, and strong acid sites, respectively [38]. The total acid sites of γ-Al_2O_3 (A0-0-01) (7.2 μmol·g^{-1}) was more than three times that of Cu–ZnO. Moreover, a ratio of strong acid sites of A0-0-01, larger than that of Cu–ZnO, was also obtained. When γ-Al_2O_3 was mixed with Cu–ZnO, the total acid sites increased along with the formation of more medium acid sites, while the ratio of strong acid sites kept relatively constant. The generation of medium acid sites may be due to the interaction between Cu–ZnO and γ-Al_2O_3 during the preparation process. The amount of strong acid sites increased with the increase in γ-Al_2O_3, in good agreement with previous reports [39].

Table 2. Acidity distribution and chemical composition of the catalysts.

Samples	Temperature of NH_3 Desportion Peaks (°C)			Acid Account for Percentage Acid Amount (μmol·g^{-1})			
	T1	T2	T3	Weak (%)	Medium (%)	Strong (%)	Total
$A_{0\text{-}0\text{-}01}$	108	275	324	50.0	36.1	13.9	7.2
$A_{4\text{-}1\text{-}00}$	103	225	333	63.6	31.8	4.5	2.2
$A_{4\text{-}1\text{-}03}$	103	224	332	66.7	30.4	2.9	10.2
$A_{4\text{-}1\text{-}05}$	102	227	335	51.9	45.7	4.9	8.1
$A_{4\text{-}1\text{-}07}$	106	225	336	47.1	48.2	4.7	8.5
$A_{4\text{-}1\text{-}10}$	105	226	334	46.5	48.8	4.7	8.6
$A_{4\text{-}1\text{-}15}$	103	225	330	46.7	47.8	5.4	9.2

2.1.4. H_2-TPR Characterization

Figure 2 shows the H_2-TPR profile of the calcined catalysts, and an asymmetrical peak can be observed. Generally, the reduction temperature of copper species changes with particle size, chemical environment, and the metal support interaction of Cu oxide species [40,41]. The intensity of reduction peak was reduced with the increased addition of γ-Al_2O_3 due to the decrease in Cu content. However, the peak area of $A_{4\text{-}1\text{-}10}$ is higher than that of $A_{4\text{-}1\text{-}07}$, although the Cu content in $A_{4\text{-}1\text{-}10}$ is lower, possibly due to the hydrogen spillover. The main reduction peak shifted from 286 °C for $A_{4\text{-}1\text{-}03}$ to 268 °C for $A_{4\text{-}1\text{-}07}$, indicating an increase in copper oxide dispersion due to the interaction between Cu–ZnO and γ-Al_2O_3. However, a further increase in the content of γ-Al_2O_3 resulted in a reduction peak at 285 °C for $A_{4\text{-}1\text{-}10}$. Evidently, the change in the H_2-TPR peak position indicated the strength of interaction (Cu–ZnO and γ-Al_2O_3), suggesting that γ-Al_2O_3 had a great impact on the copper oxide reduction. Moreover, when γ-Al_2O_3 was added to different catalysts, the reduction process of catalysts became difficult and slower. This resulted from smaller copper oxide particles or the better copper oxide dispersion on the γ-Al_2O_3 surface.

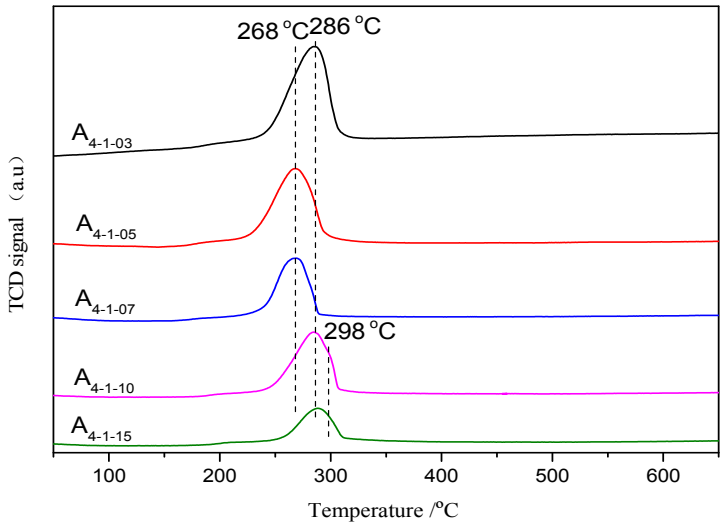

Figure 2. H_2-TPR profiles of the calcined catalyst samples.

2.1.5. HRTEM Characterization

To confirm the dispersion and morphology of catalysts particles, HRTEM images of reduced samples ($A_{4\text{-}1\text{-}00}$, $A_{4\text{-}1\text{-}10}$) were obtained (Figure 3). The dispersion of copper zinc nanoparticles was lower than that of the copper zinc aluminum catalyst. In addition, the Cu particles with sizes <30 nm were observed in the image of the copper zinc aluminum catalyst. Therefore, XRD and HRTEM results are in good agreement with each other.

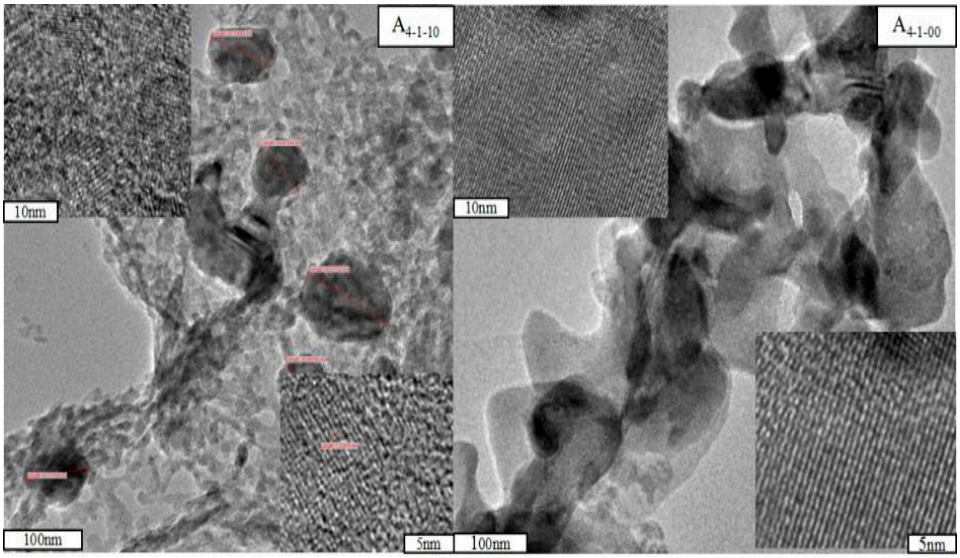

Figure 3. TEM image of the catalyst after reduction by H_2.

2.2. Catalysts Performance

2.2.1. Effect of Cu/Zn/Al Ratio

The catalytic performances of the bi-functional Cu–ZnO/Al_2O_3 catalysts are summarized in Table 3. During the catalytic conversion of THFA, reactions such as rearrangement and hydrogenation could occur, leading to the formation of DHP and THP, respectively. However, DVL and 1-pentanol represent the main by-products during the conversion of THFA, as is shown in Table 3, indicating the existence of strong acid sites. Both $A_{4\text{-}1\text{-}00}$ and $A_{0\text{-}0\text{-}01}$ showed a low conversion of THFA. The main two products over $A_{4\text{-}1\text{-}00}$ were 3,4-2H-dihydropyran (DHP) (Sel. 34.5%) and THP (Sel. 31.3%) at 255 °C and 0.6 MPa H_2, suggesting that Cu–ZnO could provide active sites for the rearrangement of THFA and further hydrogenation. In contrast, the main product was DHP over $A_{0\text{-}0\text{-}01}$ with 74.4% selectivity, indicating that the γ-Al_2O_3 could only provide acid sites for THFA rearrangement. For the Cu–ZnO/Al_2O_3 catalysts, a significant increase in THFA conversion and THP selectivity was observed compared with Cu–ZnO. Furthermore, the conversion of THFA was increased from 11.5 to 78.6%, while the selectivity of THP was improved from 31.3 to 77.8%, when the γ-Al_2O_3 content increased from $A_{4\text{-}1\text{-}00}$ to $A_{4\text{-}1\text{-}10}$. However, a further increase in alumina resulted in a decreased THFA conversion (57.4%) and THP selectivity (63.6%).

Table 3. Tetrahyrofurfuryl alcohol (THFA) conversion over different catalysts.

Catalysts	Conversion (%)	Selectivity (%)			
		THP	1-Pentanol	DVL	DHP
$A_{4\text{-}1\text{-}00}$	11.5	31.3	2.1	2.1	34.5
$A_{0\text{-}0\text{-}01}$	23.1	1.5	0.1	18.0	74.4
$A_{4\text{-}1\text{-}03}$	38.9	51.8	4.2	16.4	13.0
$A_{4\text{-}1\text{-}05}$	68.1	48.7	12.8	14.3	12.4
$A_{4\text{-}1\text{-}07}$	66.6	69.3	10.1	12.6	2.5
$A_{4\text{-}1\text{-}10}$	78.6	77.8	8.6	8.1	1.6
$A_{4\text{-}1\text{-}15}$	57.4	63.6	3.5	21.1	4.6

Reaction condition: 255 °C, 0.6 MPa, THFA: 99.9 wt %.

NH_3-TPD results suggested that γ-Al_2O_3 provided more middle and strong acid sites than Cu–ZnO. These acid sites promoted the rearrangement of THFA to DHP, and DHP can be further converted to THP at hydrogenation sites. However, δ-valerolactone (DVL) was observed as the main

byproduct over both γ-Al_2O_3 and Cu–ZnO/Al_2O_3 catalysts, while Cu–ZnO with a low content of strong acid sites showed a low selectivity of DVL. Therefore, the formation of DVL may be due to the strong acid sites. The selectivity of THP changed with the Al_2O_3 content in Cu–ZnO/Al_2O_3. Thus, the synergy between γ-Al_2O_3 (acid sites) and Cu–ZnO (metal hydrogenation sites) is the key for a high yield of THP.

In order to investigate the effects of γ-Al_2O_3 and Cu–ZnO, we compared the catalytic performance of Cu–ZnO/Al_2O_3 prepared via physical mixing and extrusion. As shown in Table 4, the THP selectivity over Cu–ZnO/Al_2O_3 prepared via extrusion was lower than that over Cu–ZnO/Al_2O_3 prepared via physical mixing at 260 °C, 0.6 MPa. However, the THP selectivity over Cu–ZnO/Al_2O_3 prepared via extrusion was obviously higher than that over Cu–ZnO/Al_2O_3 prepared via physical mixing at 280 °C, 0.6 MPa. Since the interaction between Cu–ZnO and γ-Al_2O_3 after extrusion is stronger than that after physical mixing when the temperature was higher, a strong and close interaction between hydrogenation sites (Cu–ZnO) and acid sites (γ-Al_2O_3) favored the generation of THP from THFA. Therefore, the active sites of hydrogenation and hydrogenolysis reactions were provided by metallic copper, ZnO was used as the adsorbent for THFA reaction, and the acid sites were provided by γ-Al_2O_3.

Table 4. Conversion of THFA over mechanical mixing and extrusion methods.

Catalysts	Conversion (%)	Selectivity (%)			
		THP	1-Pentanol	DVL	DHP
A [a]	57.7	68.8	4.6	18.2	3.2
B [a]	36.4	77.9	0.6	7	0.3
A [b]	98	89.5	7	0.6	0
B [b]	90.4	74.9	12	2.6	0.8

[a] Reaction condition: 240 °C, 0.6 MPa; [b] Reaction condition, 280 °C, 0.6 MPa; A: extrusion; B: mechanical mixing.

2.2.2. Effect of Reaction Temperature and H_2 Pressure

The catalytic performance of the $A_{4\text{-}1\text{-}10}$ catalyst for THFA conversion at different reaction temperatures (0.6 MPa H_2) is shown in Table 5. At a low temperature (230 °C), the selectivity for THP was 55.2%, and the main by-product was DVL. When the reaction temperature increased from 230 to 270 °C, the selectivity of THP increased rapidly from 55.2 to 91.4%. However, the selectivity of THP decreased to 85.9% after further increasing the temperature to 290 °C, due to the intensive formation of 1-pentanol. Generally, 1-pentanol was generated from excessive hydrogenolysis of THFA via the acid-catalyzed ring-opening of THP coupled with metal-catalyzed hydrogenation [42].

Table 5. Effect of reaction temperature on the conversion of THFA over $A_{4\text{-}1\text{-}10}$.

T(°C)	Conversion (%)	Selectivity (%)			
		THP	1-Pentanol	DVL	DHP
230	37.7	55.2	2.5	29	3.8
240	57.7	68.8	4.6	18.2	3.2
250	78.6	77.8	8.6	8.1	1.6
260	91.9	86.8	7.3	3	0.8
270	95.2	91.4	5.6	1.3	0.4
280	98	89.5	7	0.6	0
290	99.3	85.9	7.5	0.2	0.1

Reaction pressure: 0.6 MPa, THFA: 99.9 wt %.

Table 6 shows the effect of hydrogen pressure on the activity and selectivity in THFA hydrogenolysis over the $A_{4\text{-}1\text{-}10}$ catalyst. At low pressure (<0.4 MPa), the main by-product is DVL. When the pressure increased from 0.2 to 0.8 MPa, THFA conversion increased, while the selectivity of

THP increased from 45.5 to 90.5%. On the contrary, the DVL selectivity decreased from 17.7 to 2.6%. The changes in selectivity for THP and DVL indicated that formations of these compounds were competitive reactions. The high pressure of hydrogen promoted the generation of THP by accelerating the hydrogenation of DHP; in the meantime, the dehydrogenation of 2-HTHP was suppressed.

Table 6. Effect of pressure on the conversion of THFA over $A_{4\text{-}1\text{-}10}$.

P(MPa)	Conversion (%)	Selectivity (%)			
		THP	1-Pentanol	DVL	DHP
0.2	68.9	45.5	8.4	17.7	8.8
0.4	76.5	59.4	6.0	15.8	8.4
0.6	88.3	81.6	6.5	5.9	2.8
0.8	91.7	90.5	5.0	2.6	1.3
1.0	98.8	89.1	7.8	0.7	0.6
1.5	97.8	89.1	7.9	1.2	0.5

Reaction temperature, 250 °C, THFA: 99.9 wt %.

As shown in Figure 4, the Cu–ZnO/Al_2O_3 catalyst exhibited high activity and stability during 205 h on-stream at 270 °C and 1.0 MPa H_2. The THFA conversion and THP selectivity were 99.7% and 89.4%, respectively, after 205 h. Moreover, polymeric materials were not observed in the catalyst bed or colder parts of the unit after the stability test, suggesting that the deposit of polyesters was suppressed over the Cu–ZnO/Al_2O_3 catalyst.

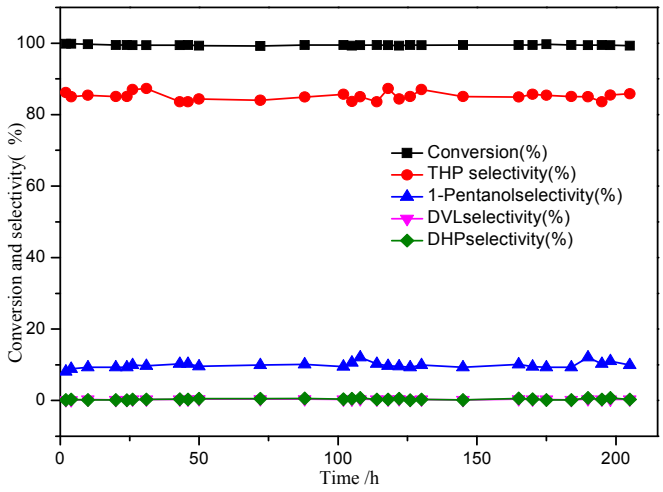

Figure 4. Catalytic stability test of Cu–ZnO/Al_2O_3 (4:1:10 = Cu/Zn/Al). (Reaction conditions: temperature, 270 °C, 1.0 MPa H_2, THFA: 99.9 wt %).

2.2.3. Reaction Paths

Scheme 1 summarizes the proposed reaction paths during the conversion of THFA to THP over Cu–ZnO/Al_2O_3, which was in good agreement with prior reports. Sato and coworkers [28] reported that the THFA could be rearranged into 2-hydroxytetrahydropyran (2-HTHP), which was then dehydrated to DHP over acid sites. In the current reaction, DHP was further converted to THP via a C=C bond hydrogenation. The effect of γ-Al_2O_3 suggested that a close interaction of metal sites and medium acid sites promoted the conversion of THFA to THP. Major by-products, such as DVL and 1-pentanol, were formed through the dehydrogenation of 2-HTHP and over-hydrogenation of THP, respectively. 1-Pentanol was generated at high temperature, and DVL was generated at low temperature and pressure. Therefore, a proper control on both temperature and pressure is needed for the suppressing of byproducts.

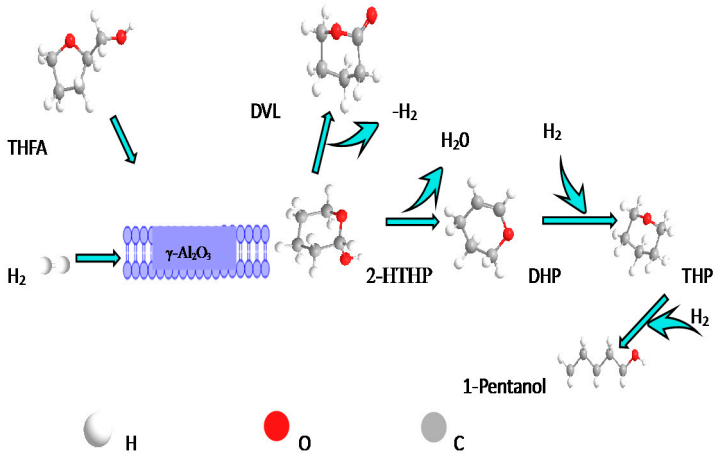

Scheme 1. Reaction pathway in the hydrogenolysis/hydrogenation of tetrahydrofurfuryl alcohol over the Cu–ZnO/Al_2O_3 catalyst in the gas phase.

3. Experimental

3.1. Catalyst Preparation

The Cu–ZnO/Al_2O_3 catalysts were prepared by means of the precipitation–extrusion method [34]. γ-Al_2O_3 produced from boehmite (>400 mesh and 26% m/m water, Shandong Aluminum Corp., Zibo, China), $Cu(NO_3)_2{\cdot}3H_2O$ (Sinopharm Chemical Reagent Co., Ltd., Shanghai, China), and $Zn(NO_3)_2{\cdot}6H_2O$ (purchased from Sinopharm Chemical Reagent Co., Ltd., Shanghai, China) were dissolved in water with a final total metal concentration of 1.4 M. Aqueous Na_2CO_3 (0.3 M) was used as a precipitating agent. During the synthesis procedure, the Na_2CO_3 solution was added dropwise to a mixed solution of Cu^{2+} and Zn^{2+} under vigorous stirring at 70 °C, and the pH was adjusted to 7.0. The resulting precipitate was then aged for 3 h at 80 °C and cooled down to room temperature. The copper/zinc carbonate precursor was obtained after filtration, washing with water for several times, and drying at 120 °C for 4 h.

Before extrusion, the boehmite was mixed with the previously prepared dried copper/zinc carbonate precursor in an Rheo-kneader at room temperature and the rotation speed was kept at 100 r·min^{-1}. The Cu/Zn/Al molar ratio (for instance, 0:0:10, 4:1:00, 4:1:03, 4:1:05, 4:1:07, 4:1:10, and 4:1:15) was modulated by changing the proportion of metal carbonates and boehmite. Herein, the Cu–ZnO/Al_2O_3 catalyst with a molar ratio of a:b:c is abbreviated as Aabc. For example, the catalyst name of "$A_{4\text{-}1\text{-}10}$" means that the molar ratio of CuO/ZnO/Al_2O_3 was 4:1:10. The paste was then submitted to a piston extruder, and cylindrical green strips with diameters of 3 mm were formed. The green strips were dried at 120 °C for 4 h before calcination at 450 °C for 5 h with a heating rate of 5 °C·min^{-1}.

3.2. Catalytic Reaction

The catalytic performance of the catalysts was investigated in a fixed-bed reactor (i.d. 20 mm, length 300 mm). The catalysts were used in cylinder state with a particle size of 3 mm in diameter. Before reaction, the calcined catalysts were reduced at 275 °C in a 20 vol % H_2/N_2 atmosphere at a flow rate of 100 mL·min^{-1} for 3 h. After that, pure THFA with hydrogen was pumped into the reactor at a rate of 0.12 mL·h^{-1}. Afterwards, the reactor was pressurized to 0.2~2.0 MPa with H_2. The reaction temperature was in the range of 230–300 °C. The liquid products were analyzed by a gas chromatography (Agilent 6890N GC, Santa Clara, CA, USA) equipped with a flame ionization

detector (FID) and an AB-FFAP capillary column (30 m × 0.32 mm × 0.25 μm). The THFA conversion and product selectivity were calculated based on the following equations:

$$\text{conversion (\%)} = (\text{moles of THFA charged-moles of THFA left})/\text{moles of THFA charged} \times 100\%$$

$$\text{selectivity (\%)} = \text{moles of a product generated}/(\text{moles of THFA charged-moles of THFA left}) \times 100\%.$$

3.3. Characterization of Catalyst

XRD data was recorded on an XRD-7000 (Kyoto, Japan) using Cu Kα radiation (λ = 0.154 nm) produced by an X-ray source and operated at 40 kV and 30 mA. A scanning angle (2θ) ranged from 10 to 80°.

The BET surface areas of the catalysts were determined through N_2 adsorption–desorption at −190 °C using a Quantachrome SI Instrument (Boynton Beach, FL, USA). Prior to measurements, all catalysts were degassed under vacuum at 100 °C for 10 min and at 300 °C for 3 h. Then, the specific surface area and BJH pore size distribution were calculated on the basis of the desorption branch of the isotherms.

The reducibility of the calcined catalysts was determined by H_2-TPR, which was conducted on an Auto Chem. II2920 (Mircromeritics, Atlanta, FA, USA). Typically, 100 mg catalysts were outgassed in N_2 at 300 °C for 1 h to remove impurities and then cooled down to room temperature. A mixture of 5 vol % H_2 and 95 vol % He was passed through the catalyst bed (20 mL·min^{-1}), while the temperature was increased from 40 to 800 °C at 15 °C·min^{-1}.

The NH_3-TPD analysis was also conducted on an Auto Chem. II 2920 (Mircromeritics, Atlanta, FA, USA). Approximately 100 mg catalysts were added to a quartz tube, pre-treated with He gas at 300 °C for 1 h, and then cooled down to room temperature. The catalysts were saturated with pure NH_3 for 1 h. The samples were then cleaned with He gas at 50 °C to remove the physically adsorbed NH_3. During the measurement, the temperature was raised to 800 °C at 10 °C·min^{-1} with the flow of He (50 mL·min^{-1}) to desorb NH_3. TEM were investigated using a JEM-2100F electron microscope (Akishima, Tokyo, Japan) at 200 kV.

4. Conclusions

The highly selective vapor-phase hydrogenolysis of THFA to THP was realized over a Cu–ZnO/Al_2O_3 catalyst prepared via precipitation–extrusion. The yield of THP is closely related to the ratio of Cu/Zn/Al, reaction temperature, and H_2 pressure. At 270 °C and 1.0 MPa H_2, the THP selectivity from THFA was up to 89.4% over the optimum Cu–ZnO/Al_2O_3 catalyst (the molar ratio of Cu/Zn/Al being 4:1:10). During the conversion of THFA to THP, it was found that three consecutive reactions were involved: (1) the rearrangement of THFA into 2-HTHP, (2) the dehydration of 2-HTHP to DHP, and (3) the hydrogenation of DHP to THP. The synergy of metal sites and medium acid sites is the key for a high catalytic activity for the production of THP from THFA.

Supplementary Materials: The supplementary materials are available online at www.mdpi.com/2073-4344/8/3/105/s1, Table S1: the comparison of results THF and THP as solvent, Figure S1: Particle volume-size distribution of the Cu-ZnO/Al2O3 catalysts, Figure S2: N2 physisorption isotherm of the Cu-ZnO/Al2O3 catalysts, Figure S3: NH3-TPD patterns of Cu-ZnO/Al2O3 catalysts with different γ-Al2O3.

Acknowledgments: This project was supported by the Beijing Natural Science Foundation (2184101).

Author Contributions: F.Z., B.Z. and L.H. conceived and designed the experiments; F.Z. performed the experiments; F.Z., X.W., L.H. and D.J., analyzed the data; S.D. and S.L. contributed materials and analysis tools; F.Z., B.Z., X.W., L.H. and L.M. wrote the paper.

Conflicts of Interest: The authors declare no conflict of interest.

References

1. Corma, A.; Sara Iborra, A.; Velty, A. Chemical Routes for the Transformation of Biomass into Chemicals. *Chem. Rev.* **2007**, *107*, 2411–2502. [CrossRef] [PubMed]
2. Gallezot, P. Conversion of biomass to selected chemical products. *Chem. Soc. Rev.* **2012**, *41*, 1538–1558. [CrossRef] [PubMed]
3. Li, C.; Zhao, X.; Wang, A.; Huber, G.W.; Zhang, T. Catalytic Transformation of Lignin for the Production of Chemicals and Fuels. *Chem. Rev.* **2015**, *115*, 11559. [CrossRef] [PubMed]
4. Karinen, R.; Vilonen, K.; Niemelä, M. Biorefining: Heterogeneously Catalyzed Reactions of Carbohydrates for the Production of Furfural and Hydroxymethylfurfural. *ChemSusChem* **2011**, *4*, 1002–1016. [CrossRef] [PubMed]
5. Agirrezabal-Telleria, I.; Hemmann, F.; Jäger, C.; Arias, P.L.; Kemnitz, E. Functionalized partially hydroxylated MgF_2, as catalysts for the dehydration of d-xylose to furfural. *J. Catal.* **2013**, *305*, 81–91. [CrossRef]
6. Yan, K.; Wu, G.; Lafleur, T.; Jarvis, C. Production, properties and catalytic hydrogenation of furfural to fuel additives and value-added chemicals. *Renew. Sustain. Energy Rev.* **2014**, *38*, 663–676. [CrossRef]
7. Besson, M.; Gallezot, P.; Pinel, C. Conversion of Biomass into Chemicals over Metal Catalysts. *Chem. Rev.* **2014**, *114*, 1827–1870. [CrossRef] [PubMed]
8. Nakagawa, Y.; Tomishige, K. Catalyst Development for the Hydrogenolysis of Biomass-Derived Chemicals to Value-Added Ones. *Catal. Surv. Asia* **2011**, *15*, 111–116. [CrossRef]
9. Nakagawa, Y.; Tomishige, K. Production of 1, 5-pentanediol from biomass via furfural and tetrahydrofurfuryl alcohol. *Catal. Today* **2012**, *195*, 136–143. [CrossRef]
10. Nakagawa, Y.; Tamura, M.; Tomishige, K. Catalytic Reduction of Biomass-Derived Furanic Compounds with Hydrogen. *ACS Catal.* **2013**, *3*, 2655–2668. [CrossRef]
11. Tomishige, K.; Tamura, M.; Nakagawa, Y. Role of Re species and acid cocatalyst on Ir-ReO_x/SiO_2 in the C–O hydrogenolysis of biomass-derived substrates. *Chem. Rec.* **2014**, *14*, 1041–1054. [CrossRef] [PubMed]
12. Nakagawa, Y.; Nakazawa, H.; Watanabe, H. Total Hydrogenation of Furfural over a Silica-Supported Nickel Catalyst Prepared by the Reduction of a Nickel Nitrate Precursor. *ChemCatChem* **2012**, *4*, 1791–1797. [CrossRef]
13. Koso, S.; Furikado, I.; Shimao, A.; Miyazawa, T.; Kunimori, K.; Tomishige, K. Chemoselective hydrogenolysis of tetrahydrofurfuryl alcohol to 1,5-pentanediol. *Chem. Commun.* **2009**, *15*, 2035–2037. [CrossRef] [PubMed]
14. Koso, S.; Ueda, N.; Shinmi, Y.; Okumura, K.; Kizuka, T.; Tomishige, K. Promoting effect of Mo on the hydrogenolysis of tetrahydrofurfuryl alcohol to 1,5-pentanediol over Rh/SiO_2. *J. Catal.* **2009**, *267*, 89–92. [CrossRef]
15. Koso, S.; Nakagawa, Y.; Tomishige, K. Mechanism of the hydrogenolysis of ethers over silica-supported rhodium catalyst modified with rhenium oxide. *J. Catal.* **2011**, *280*, 221–229. [CrossRef]
16. Chia, M.; Pagán-Torres, Y.J.; Hibbitts, D.; Tan, Q.; Pham, H.N.; Datye, A.K.; Neurock, M.; Davis, R.J.; Dumesic, J.A. Selective hydrogenolysis of polyols and cyclic ethers over bifunctional surface sites on rhodium-rhenium catalysts. *J. Am. Chem. Soc.* **2011**, *133*, 12675–12689. [CrossRef] [PubMed]
17. Chen, K.; Mori, K.; Watanabe, H.; Nakagawa, Y.; Tomishige, K. C–O bond hydrogenolysis of cyclic ethers with OH groups over rhenium-modified supported iridium catalysts. *J. Catal.* **2012**, *294*, 171–183. [CrossRef]
18. Koso, S.; Watanabe, H.; Okumura, K.; Nakagawa, Y.; Tomishige, K. Comparative study of Rh–MoO_x and Rh–ReO_x supported on SiO_2 for the hydrogenolysis of ethers and polyols. *Appl. Catal. B Environ.* **2012**, *111*, 27–37. [CrossRef]
19. Nakagawa, Y.; Mori, K.; Chen, K.; Amada, Y.; Tamura, M.; Tomishige, K. Hydrogenolysis of C, O bond over Re-modified Ir catalyst in alkane solvent. *Appl. Catal. A Gen.* **2013**, *468*, 418–425. [CrossRef]
20. Liu, S.; Amada, Y.; Tamura, M.; Nakagawa, Y.; Tomishige, K. Performance and characterization of rhenium-modified Rh–Ir alloy catalyst for one-pot conversion of furfural into 1,5-pentanediol. *Catal. Sci. Technol.* **2014**, *4*, 2535–2549. [CrossRef]
21. Liu, S.; Amada, Y.; Tamura, M.; Nakagawa, Y.; Tomishige, K. One-pot selective conversion of furfural into 1, 5-pentanediol over a Pd-added Ir–ReO_x/SiO_2 bifunctional catalyst. *Green Chem.* **2014**, *16*, 617–626. [CrossRef]
22. Pholjaroen, B.; Li, N.; Huang, Y.; Li, L.; Wang, A.; Zhang, T. Selective hydrogenolysis of tetrahydrofurfuryl alcohol to 1,5-pentanediol over vanadium modified Ir/SiO_2, catalyst. *Catal. Today* **2015**, *245*, 93–99. [CrossRef]

23. Feng, S.; Nagao, A.; Aihara, T.; Miura, H.; Shishido, T. Selective hydrogenolysis of tetrahydrofurfuryl alcohol on Pt/WO_3/ZrO_2, catalysts: Effect of WO_3, loading amount on activity. *Catal. Today* **2017**, *303*, 207–212. [CrossRef]
24. Wan, W.; Jenness, G.R.; Xiong, K.; Vlachos, D.G.; Chen, J.G. Ring-Opening Reaction of Furfural and Tetrahydrofurfuryl Alcohol on Hydrogen-Predosed Iridium(III) and Cobalt/Iridium(III) Surfaces. *ChemCatChem* **2017**, *9*, 1701–1707. [CrossRef]
25. Brentzel, Z.J.; Barnett, K.J.; Huang, K.; Maravelias, C.T.; Dumesic, J.A.; Huber, G.W. Chemicals from Biomass: Combining Ring-Opening Tautomerization and Hydrogenation Reactions to Produce 1, 5-Pentanediol from Furfural. *ChemSusChem* **2017**, *10*, 1351–1355. [CrossRef] [PubMed]
26. Schniepp, L.E.; Geller, H.H. Preparation of Dihydropyran, δ-Hydroxyvaleraldehyde and 1,5-Pentanediol from Tetrahydrofurfuryl Alcohol. *J. Am. Chem. Soc.* **1946**, *68*, 1646–1648. [CrossRef] [PubMed]
27. Wilson, C.L. Reactions of Furan Compounds. VII. Thermal Interconversion of 2,3-Dihydrofuran and Cyclopropane Aldehyde. *J. Am. Chem. Soc.* **1947**, *69*, 3002–3004. [CrossRef]
28. Sato, S.; Igarashi, J.; Yamada, Y. Stable vapor-phase conversion of tetrahydrofurfuryl alcohol into 3, 4–2 H -dihydropyran. *Appl. Catal. A Gen.* **2013**, *453*, 213–218. [CrossRef]
29. Thomas, H.P.; Wilson, C.L. Reactions of Furan Compounds. XV. Behavior of Tetrahydrofurfuryl Alcohol over Iron-Copper Catalysts. *J. Am. Chem. Soc.* **2002**, *73*, 4803–4805. [CrossRef]
30. Sato, S.; Takahashi, R.; Yamamoto, N.; Kaneko, E.; Inoue, H. Vapor-phase dehydration of 1,5-pentanediol into 4-penten-1-ol. *Appl. Catal. A Gen.* **2008**, *334*, 84–91. [CrossRef]
31. Yamaguchi, A.; Hiyoshi, N.; Sato, O.; Bando, K.K.; Shirai, M. Enhancement of cyclic ether formation from polyalcohol compounds in high temperature liquid water by high pressure carbon dioxide. *Green Chem.* **2009**, *11*, 48–52. [CrossRef]
32. Agrawal, O. *Organic Chemistry Reactions and Reagents*; Goel Publishing House: New Delhi, India, 2008; Volume 627, pp. 686–687.
33. Falbe, J. *Carbon Monoxide in Organic Synthesis*; Springer: Berlin/Heidelberg, Germany, 1970.
34. Müller, S.P.; Kucher, M.; Ohlinger, C.; Kraushaar-Czarnetzki, B. Extrusion of Cu/ZnO catalysts for the single-stage gas-phase processing of dimethyl maleate to tetrahydrofuran. *J. Catal.* **2003**, *218*, 419–426. [CrossRef]
35. Guo, P.J.; Chen, L.F.; Yan, S.R.; Dai, W.L.; Qiao, M.H.; Xu, H.L.; Fan, K.N. One-step hydrogenolysis of dimethyl maleate to tetrahydrofuran over chromium-modified Cu–B/γ-Al_2O_3, catalysts. *J. Mol. Catal. A Chem.* **2006**, *256*, 164–170. [CrossRef]
36. Soghrati, E.; Choong, C.; Poh, C.K.; Kawi, S.; Borgna, A. Single-Pot Conversion of Tetrahydrofurfuryl Alcohol into Tetrahydropyran over a Ni/HZSM—5 Catalyst under Aqueous-Phase Conditions. *ChemCatChem* **2017**, *9*, 1402–1408. [CrossRef]
37. Gong, J.; Yue, H.; Zhao, Y.; Zhao, S.; Zhao, L.; Lv, J.; Wang, S.; Ma, X. Synthesis of Ethanol via Syngas on Cu/SiO_2 Catalysts with Balanced Cu^0–Cu^+ Sites. *J. Am. Chem. Soc.* **2012**, *134*, 13922. [CrossRef] [PubMed]
38. Atia, H.; Armbruster, U.; Martin, A. Dehydration of glycerol in gas phase using heteropolyacid catalysts as active compounds. *J. Catal.* **2008**, *258*, 71–82. [CrossRef]
39. Zhu, Y.; Kong, X.; Li, X.; Ding, G.; Zhu, Y.; Li, Y. Cu Nanoparticles Inlaid Mesoporous Al_2O_3 As a High-Performance Bifunctional Catalyst for Ethanol Synthesis via Dimethyl Oxalate Hydrogenation. *ACS Catal.* **2014**, *4*, 3612–3620. [CrossRef]
40. Huang, Z.W.; Cui, F.; Xue, J.J.; Zuo, J.; Chen, J.; Xia, C. Cu/SiO_2 catalysts prepared by hom- and heterogeneous deposition-precipitation methods: Texture, structure, and catalytic performance in the hydrogenolysis of glycerol to 1,2-propanediol. *Catal. Today* **2012**, *183*, 42–51. [CrossRef]
41. Burattin, P.; Che, M.; Louis, C. Molecular Approach to the Mechanism of Deposition−Precipitation of the Ni(II) Phase on Silica. *J. Phys. Chem. B* **1998**, *102*, 2722–2732. [CrossRef]
42. Herrmann, U.; Emig, G. Liquid phase hydrogenation of maleic anhydride and intermediates on copper-based and noble metal catalysts. *Ind. Eng. Chem. Res.* **1997**, *36*, 2885–2896. [CrossRef]